2.5-THz GaAs Monolithic Membrane-Diode Mixer

Peter H. Siegel, *Senior Member, IEEE,* R. Peter Smith, Michael C. Gaidis, and Suzanne C. Martin, *Associate Member, IEEE*

***Abstract*— A novel GaAs monolithic membrane-diode (MOMED) structure has been developed and implemented as a 2.5-THz Schottky diode mixer. The mixer blends conventional machined metallic waveguide with micromachined monolithic GaAs circuitry to form, for the first time, a robust, easily fabricated, and assembled room-temperature planar diode receiver at frequencies above 2 THz. Measurements of receiver performance, in air, yield a $T_{\rm receiver}$ of 16 500-K double sideband (DSB) at 8.4-GHz intermediate frequency (IF) using a 150-K commercial Miteq amplifier. The receiver conversion loss (diplexer through IF amplifier input) measures 16.9 dB in air, yielding a derived "front-end" noise temperature below 9000-K DSB at 2514 GHz. Using a CO_2-pumped methanol far-infrared laser as a local oscillator at 2522 GHz, injected via a Martin–Puplett diplexer, the required power is $\approx$5 mW for optimum pumping and can be reduced to less than 3 mW with a 15% increase in receiver noise. Although demonstrated as a simple submillimeter-wave mixer, the all-GaAs membrane structure that has been developed is suited to a wide variety of low-loss high-frequency radio-frequency circuits.**

***Index Terms*—FIR, GaAs, membrane, micromachined, planar, radiometer, Schottky diode mixer, THz, waveguide.**

I. Introduction

The terahertz frequency range offers a unique challenge for both heterodyne circuit and device designers. It represents a crossover regime where wavelength scales stretch the tolerances of traditional machining as well as the dimensions and geometries accessible through photolithographic processes. In addition, critical device and radio-frequency (RF) circuit dimensions require submicrometer resolution to reduce parasitics, whereas surrounding circuitry, especially at the intermediate frequencies which lie in the microwave bands, require macroscopic structures with smooth mechanical and electronic transitions to the RF environment. In this paper, we report on a process and component design which blends the flexibility of mechanical machining with the tight tolerances and multiple die processing advantages of micromachining. Although the techniques and circuit concepts described in this paper have been aimed at a specific NASA spaceflight component realization, a 2.5-THz Schottky diode mixer, other millimeter and submillimeter-wave GaAs semiconductor circuits can be enhanced with similar processing: frequency multipliers, detectors, oscillators, antenna coupled devices, planar array circuits, etc. The mixture of semiconductor and mechanical fabrication techniques, blending of the active device and surrounding passive RF circuitry, enhanced reliability and ease of handling of the planar circuit, and solid RF performance achieved with the first demonstration circuit have opened a new window of opportunity for submillimeter-wave semiconductor circuitry.

Manuscript received July 1, 1998; revised November 20, 1998. This work was supported by the National Aeronautics and Space Administration's Office of Advanced Concepts and Technology under a contract and by the Earth Observing System Microwave Limb Sounder Project Office.

The authors are with the California Institute of Technology, Jet Propulsion Laboratory, Pasadena, CA 91109 USA.

Publisher Item Identifier S 0018-9480(99)03130-0.

II. GaAs Membrane

A. Introduction and Concept

Due to moding effects, high-frequency circuits are often limited by the thickness of the support substrates that must be used to define the active and passive RF structures employed for signal processing. After device and circuit processing, microwave semiconductor substrates are generally mechanically lapped to a thickness as small as 50 μm; but even 50 μm is too thick for microstrip circuits above 300 GHz. Also, III–V semiconductors like GaAs are extremely brittle, and handling is a major problem with these wafer dimensions. Wet chemical etching has been used to thin GaAs-based devices to a thickness of <5 μm, but here again, handling and cracking of the substrate material becomes a major concern.

Silicon micromachining techniques have been used very successfully to make a variety of RF structures and components, including superconducting mixers, with dimensions compatible with terahertz circuitry [1]–[6]. However, these components rely on the mechanical, not electrical, properties of the silicon for their applications. At high frequencies, silicon cannot be used to form good quality active devices, i.e., diodes, transistors, etc. For device applications above 50 GHz, III–V semiconductors, particularly GaAs, are preferred over silicon. Several research groups [7]–[10] have recently investigated GaAs membrane structures. These approaches have led to techniques for fabricating GaAs membranes of multiple shapes and sizes for a few assorted mechanical applications. Although some device incorporation has been attempted [8], [11], no one has yet taken advantage of the combined device/RF properties afforded by a GaAs membrane technology or realized a membrane fabrication approach that is compatible with existing high-frequency circuits and devices.

The GaAs membrane process we report in this paper is tailored specifically for compatibility with existing RF circuit and two-terminal device realizations at terahertz frequencies. It is a relatively straightforward process, requires no strongly anisotropic etchants, makes use of a simple epitaxial layer structure with two AlGaAs etch stops, and is directly compatible with an existing terahertz planar diode fabrication process [12].

0018–9480/99$10.00 © 1999 IEEE

Top junction layer n GaAs (1000Å, doped 1e18)
Buried Ohmic layer n+ GaAs (1μm, doped 5e18)
Top Etch Stop (600Å, Al .55 Ga .45 As)
Membrane Layer (semi-insulating, 3μm)
Bottom Etch Stop (4000Å, Al.55 Ga .45 As)
GaAs Substrate (lapped to 50 μm after top-side processing)

Fig. 1. Wafer profile for membrane and device/RF circuit definition. Layer pattern (from top): n doped GaAs, n^+ GaAs, AlGaAs etch stop (device definition) followed by semi-insulating GaAs (membrane layer), AlGaAs etch stop, and host wafer (used to form frames).

B. Diode and Membrane Fabrication

The 2.5-THz mesa air-bridge T-anode Schottky barrier diodes used for the mixer circuit described in this paper are fabricated in a process which is similar to one developed for terahertz resonant tunneling diodes [13] with a few enhancements and a novel planarization step. In order to allow subsequent membrane formation, the GaAs host wafer has the epitaxial structure shown in Fig. 1. The only additional layer structures required over our traditional mesa Schottky diodes are the 3-μm-thick semi-insulating layer and the lower etch stop which define the membrane. All device and surrounding RF circuit processes are completed before membrane definition occurs.

Front-side lithography is defined using a combination of tools including a 5× I-line projection mask aligner, 50-kV electron-beam system, and contact lithography. Conventional recessed Au/Ge/Ni/Ag/Au ohmic contacts are used. Two mesas are required for each device because of our anode process [12], [13]. The active mesa is slightly larger ($\approx$1 μm) than the ohmic contact, and it is etched using a selective $BCl_3/SF_6/Ar$ mixture in an electron cyclotron resonance (ECR) reactive ion-etch (RIE) system. 0.5 μm of gold is used to provide air-bridges to the tops of the vertical mesa walls and to form the RF filters and the intermediate frequency (IF) and dc bias lines used to connect the diode with off-chip mixer circuitry.

Anodes are formed using a novel polymethyl methacrylate (PMMA) quasi-planarization technique followed by a PMMA/copolymer/PMMA trilayer resist process as is commonly used for high electron-mobility transistor (HEMT) or field-effect transistor (FET) T-gates [13]. The PMMA planarization is done by spinning on multiple layers of 495-k PMMA to a thickness of approximately 4–5 μm, much thicker than the height of the mesas, followed by a sequence of deep-UV blanket exposures and brief acetone spin-develop steps until the mesa tops are exposed. PMMA was chosen for the planarization because more commonly used substances turned out to be incompatible with the PMMA used for the anode lithography. The definition of the Ti/Pt/Au anodes has been described elsewhere [14]. Finally, plasma-enhanced chemical-vapor deposition (PECVD) silicon nitride is used to passivate the finished devices.

The first membrane-related processing step lithographically defines the membrane strips from the top side of the wafer. CF_4/O_2 RIE is used to remove the silicon–nitride device passivation layer. An ECR system using BCl_3/Ar, then BCl_3/SF_6/Ar, is used to continue etching down to the lower AlGaAs etch stop layer. Material must be left wherever the membranes themselves are to be formed, as well as over the tops of the frames so that there is no step in the metallization layer as it traverses the frame.

The wafer is next mounted top-side down, using wax, onto a suitable carrier wafer, e.g., silicon, glass, or sapphire. The backside is then lapped and polished to the desired frame thickness of 50 μm. After lapping, the backside of the wafer is cleaned by subjecting it to a light etch and then protected by a low-temperature deposited (ECR) silicon–nitride layer. The back of the wafer is then coated with photoresist and, employing a backside aligner, the relative positioning of the membrane and support frame is accomplished. The silicon nitride is then etched from all nonframe areas, including all membrane areas, by RIE.

The frames are then formed by wet etching in an H_2O_2/NH_3OH mixture [15] that selectively etches GaAs relative to AlGaAs. A brief nonselective etch (phosphoric acid/hydrogen peroxide/water) is then used to remove the AlGaAs etch stop. An additional lithography step and dry etch can be employed to expose metal beam leads overhanging the edges of the frames when such leads are desired.

The membranes with their associated RF structures and frames are now completely defined. The finished parts can be removed from the carrier wafer by dissolving the wax and any remaining photoresist in an appropriate solvent. The parts can be collected in a fine mesh placed in the bottom of the solvent vessel. No dicing or cleaving of the final parts is required. Process steps are shown in Fig. 2 and SEM micrographs of the finished parts are shown in Fig. 3.

III. 2.5-THz Mixer

A. Introduction and Concept

The lowest order OH doublets at 2510 and 2514 GHz are strong tracers for the reaction rates of key ozone depleting cycles in the Earth's atmosphere. By a fortuitous coincidence of nature, a strong methanol laser line at 2522 GHz can be used as a pump source for heterodyning; producing intermediate frequencies (IF's) at 8 and 12 GHz. An O_2 line at 2502 GHz provides a convenient pressure (altitude pointing) calibration at an IF of 20 GHz. A receiver noise temperature of 20 000-K single-sideband provides enough sensitivity to allow daily global stratospheric maps of OH above 35 km and weekly zonal maps above 18 km from a satellite in polar orbit. State-of-the-art room-temperature Schottky diode mixers approach this performance level.

Whisker-contacted corner-cube mixers have been used at frequencies at and above 2.5 THz for many years [see, e.g., 16–19]. Although the performance that has been reported [18] can be exceptionally good, the corner-cube suffers from the following three major drawbacks:

1) low reliability;
2) poor beam quality;

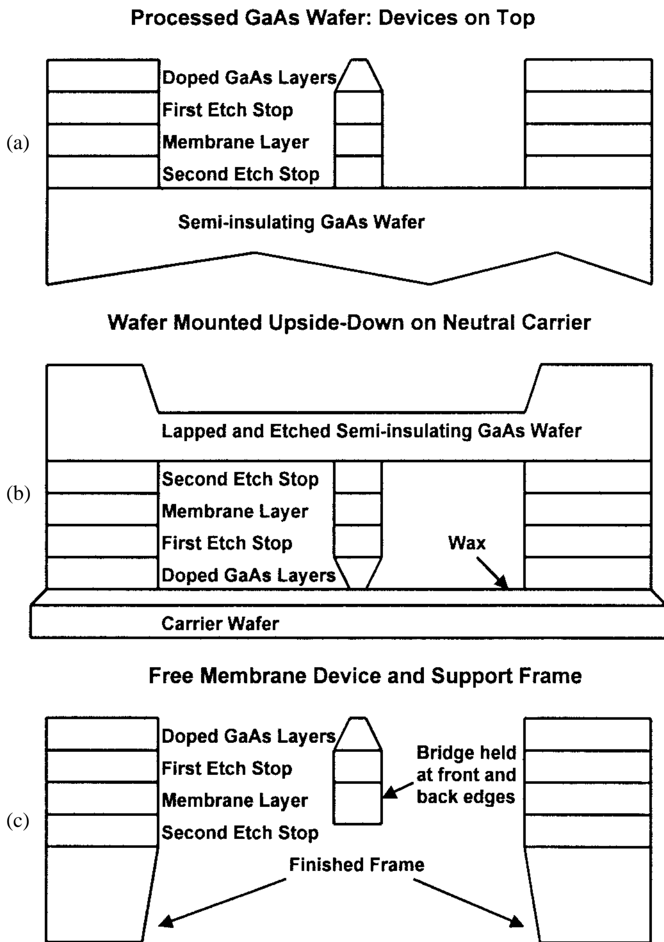

Fig. 2. Membrane fabrication steps. (a) Finished top-side wafer (with devices and RF circuitry) is etched down to lower etch stop, defining membrane region. (b) Wafer is mounted upside down on carrier using low temperature wax. Wafer is thinned, frame is patterned and etched out to bottom of membrane. (c) Etch stop is removed, wax is dissolved, individual membranes and frame float off carrier and are collected by filter or screen at bottom of beaker.

3) extremely tight assembly tolerances that substantially affect RF performance and beam shape.

Recently, a group at Rutherford Appleton Laboratory, Didcot, U.K., fabricated waveguide-based 2.5-THz mixers with a novel "planar-whisker" contact and excellent noise performance [20], [21]. They also proposed a means to integrate the diode and whisker contact into a fully planar circuit coupled to a photolithographically defined waveguide [22]. Drawing on this concept, but using a somewhat different circuit approach, the monolithic membrane diode (MOMED) integrated into a mechanically machined waveguide circuit, we have achieved the same goals of high reliability, state-of-the-art performance, and ease of assembly.

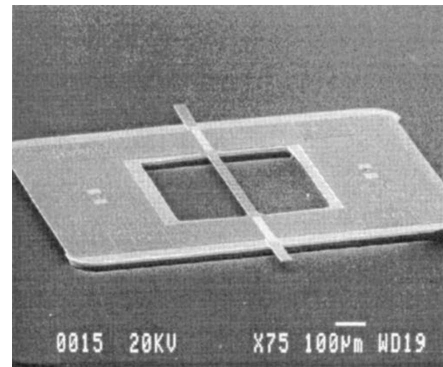

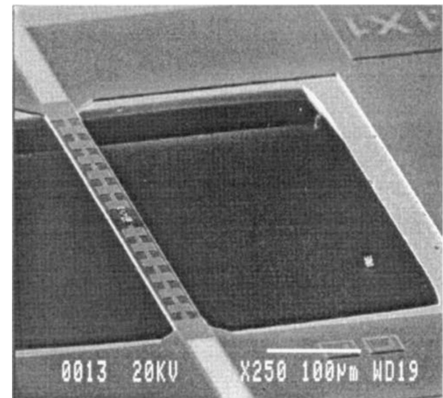

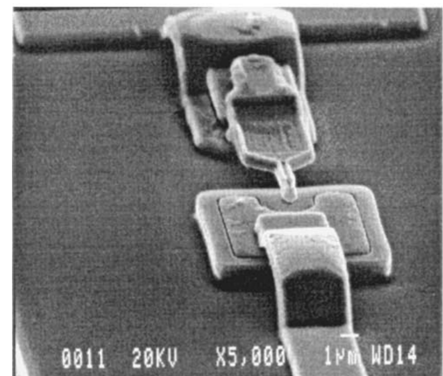

Fig. 3. SEM micrographs of completed membrane and frame with 2.5-THz Schottky diode and RF low-pass filter structure. Frame dimensions are 1 mm $\times$ 1.4 mm $\times$ 50 μm thick. Membrane is 36 μm $\times$ 600 μm $\times$ 3 μm thick.

B. Mixer Design and Fabrication

The mixer design is based upon a scaling of lower frequency single-ended mixer circuits with modifications that allow for relatively simple fabrication and assembly at 2.5 THz. Since the intended application is a space-based instrument, special consideration is given to device and circuit reliability and performance repeatability.

The mixer consists of the following five pieces:

1) MOMED, which contains all RF filter circuitry;
2) electroformed "button-mount" that houses the membrane and a single-mode 2.5-THz signal waveguide and feed horn;
3) interchangeable fixed-depth hobbed backshort section;
4) fused quartz suspended-substrate IF transformer;
5) split-block housing that holds the RF and IF pieces as well as dc bias resistors and dc and IF connectors.

A separate IF amplifier is required, as well as an appropriate RF diplexer for local oscillator (LO) injection.

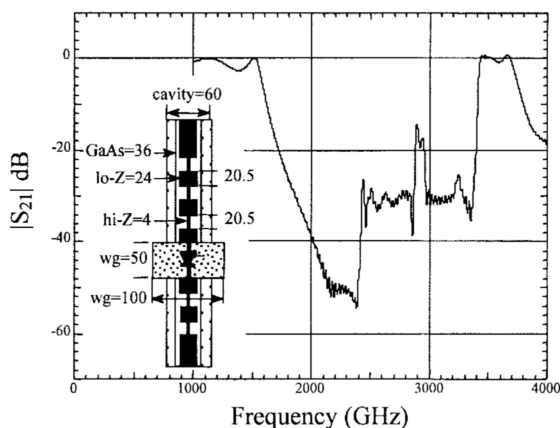

Fig. 4. Calculated FDTD performance of a four-section RF choke with dimensions equal to those in the existing device. The inset shows a dimensioned (in micrometers) top view of the membrane strip as mounted. The cavity depth is 40 μm. A more ideal configuration would utilize a 30-μm cavity depth and a 30-μm-wide GaAs membrane strip, as asymmetries in the membrane mounting would be less likely to induce undesired mode propagation.

The MOMED's unique bridge structure (Fig. 3) allows placement of the diode across the center of the broad wall of the 2.5-THz waveguide. Surrounding the diode on the membrane are low-pass filters, which both block RF propagation from the waveguide port. Unlike the configuration described in [2], the thin (36-μm wide, 600-μm long) membrane bridge is actually suspended along the centerline of a sealed single-mode transmission-line cavity (60-wide μm $\times$ 40-μm-high cross section, metal on all sides) forming a 3-μm-thick GaAs suspended stripline circuit. The membrane support frame lies outside the sealed cavity (active RF area) and is intended to have no effect on the signal coupling. A finite-difference time-domain (FDTD) analysis [23] of the filter is shown in Fig. 4. An interesting result of the analysis was the appearance at the center of the stop band of what we believe is a propagating ridge waveguide mode between the membrane and cavity side. This mode could only be reliably suppressed by reducing the height of the stripline cavity from 60 to $<$40 μm, hence, the resulting asymmetric cross section.

The membrane thickness (3 μm) was chosen as a compromise between ease of fabrication (epitaxial growths of $>$4 μm are expensive) and mechanical robustness. Careful adjustment of the membrane layer thickness to avoid mechanical stress (a concern in silicon–nitride membrane configurations) does not appear to be necessary. In our tests, a membrane thickness of 3 μm gave sufficient robustness to a 600-μm-long 36-μm-wide beam. No strain-related bowing was visible, even after device and metal deposition. Membranes of 1.2- and 2-μm thickness with widths varying between 10 and 80 μm were also fabricated on test wafers, and although they survived routine handling and had no signs of mechanical stress, the thicker membrane structure was deemed more reliable for spaceflight applications.

The length of the membrane bridge was chosen to be as short as possible and still accommodate sufficient high/low impedance filter sections for reasonable RF rejection. The membrane frame size was selected to be large enough for handling, yet small enough to have a negligible effect at the highest IF frequency (21 GHz). The diode epitaxial layer properties and anode area were selected to minimize parasitic effects without severely compromising the diode nonlinearity (ideality factor no higher than 1.5). Initial wafer variations included only anode area (0.2 μm $\times$ 1 μm and 0.35 μm $\times$ 1 μm), anode finger shape (an S-bend was included in case stress on the membrane turned out to be a problem; it did not) and required process variation bracketing. A membrane variation which included overhanging beam leads (for IF and dc bonding) was also included.

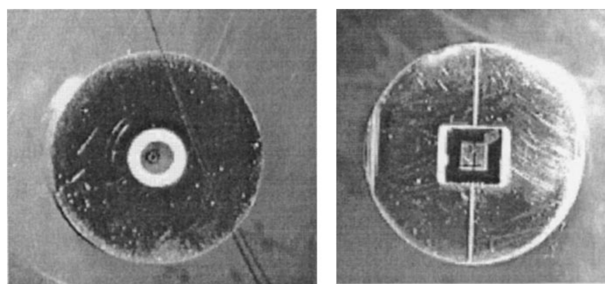

Fig. 5. 2.5-THz electroformed "button-mount" showing horn aperture (with human hair) on one side and 2.5-THz waveguide with inserted membrane mixer MOMED on the other.

Upon completion of the membrane fabrication process, the separated circuits are collected on filter paper, transferred *en masse* to a wafer holder, and individually probed and sorted before being inserted into the mixer block. Device yield on the first quarter wafer run was fairly poor with only about 10% of the diodes surviving with good dc performance characteristics (series resistance below 20 Ω, leakage current below 5 μA). Through process modifications, yield on subsequent runs was improved to approximately 30%.

Mechanically, almost all the membrane structures survived intact and there is no observed strain or strain-related problems. Device reliability appears to be very high, although no Arrhenius tests have as yet been completed. Sample devices were thermally cycled from -50 to $+150$ C (ten cycles, 15-min dwell) with no observed changes in their dc characteristics. Devices were also subjected to vibration (13 g(rms), 20 Hz to 2 kHz) with no degradation. During device mounting, the membrane frames are picked up, dropped into place in the mixer block, glued with cyanoacrylic, and probed, all with no apparent detrimental effects.

The RF coupling circuit, which provides signal and LO to the membrane diode, is formed in a standard copper electroforming operation. This electroformed "button mount" (Fig. 5) contains a single-mode 2.5-THz rectangular waveguide (nominally 100 μm $\times$ 50 μm), a tapered transition to circular waveguide, and a scaled Pickett–Potter dual-mode feed horn [24] (aluminum mandrel shown in Fig. 6).

Other than the small waveguide dimensions, no special requirements are placed on the fabrication at this point. Following electroforming, but while the aluminum mandrel still fills the waveguide cavity, the button mount is machined to final size (0.187 in $\times$ 0.075 in). A relief cavity to house the membrane frame is then milled into the copper and the suspended stripline filter cavity is machined across the button and through the center of the waveguide using a high-speed

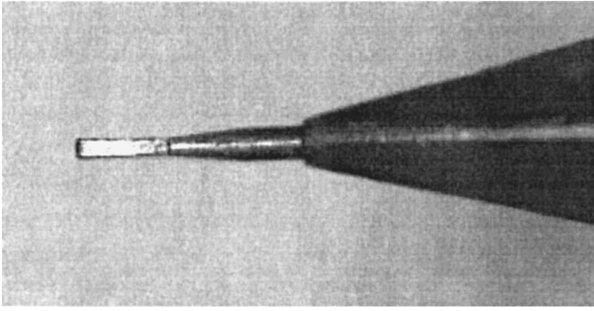

Fig. 6. 2.5-THz Pickett–Potter feed-horn mandrel. Tip dimensions are 50 μm × 100 μm. Mandrel is etched away in NaOH after electroforming.

diamond saw with a cubic boron–nitride loaded blade. The depth of the stripline cavity channel is set at this time to precisely locate the membrane bridge and frame below the surface of the button, at a depth determined by two support ledges that have been machined into the frame relief slot. These ledges catch and support the bottom of a membrane web left between dog ears on both sides of the membrane frame. Since the ledge references the membrane itself, it precisely positions the suspended stripline filter vertically in the enclosed cavity. After dicing the stripline slot, the aluminum mandrel is etched out of the copper button using NaOH.

The button is press fit into a brass split-block mount that also contains a much larger stripline cavity to house the IF transformer and the bias and IF connectors. Machining of this portion of the mixer block is straightforward.

In order to provide some degree of adjustable matching to the diode, a fixed-depth backshort cavity, aligned with the 2.5-THz waveguide, is added over the top of the membrane. Since the membrane frame support ledges locate the membrane and the top of the frame below the top surface of the button mount, the waveguide and stripline cavity are completely sealed off by the backshort cavity block. The backshort cavity itself is easily formed using a hobbing technique to punch the rectangular hole to depths as great as several mils. A range of cavity depths is readily obtained by hobbing deeper than required slots in individual holders, then finishing with a few strokes on some fine lapping paper to reach the desired depth. Alignment of the blind waveguide in the backshort piece with the waveguide in the button mount is accomplished by picking up alignment holes in both parts under an optical microscope. The fixed backshort feature makes tuning rather time consuming, but assures extremely stable and repeatable measurements and requires no changes for flight implementation. Optimal cavity depth so far varies only by a few micrometers for different diodes of the same nominal anode size.

The final piece of the mixer block is the IF transformer which converts the expected diode output impedance of 200–250 Ω to 50 Ω over the required IF bandwidth of 7–21 GHz. In order to be mechanically and electrically compatible with the tiny membrane structure and, at the same time, provide a very high impedance to the output of the GaAs filter, a thin (125 μm) fused quartz, suspended stripline transformer design was selected. The stripline cavity is sized

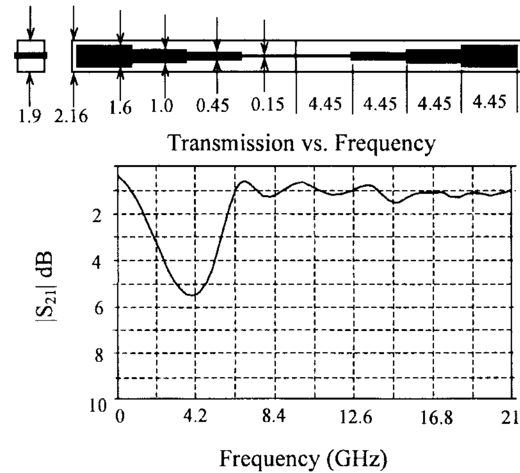

Fig. 7. Dimensioned diagram (in millimeters) and HP8510 plot of transmission loss for two back-to-back 7–21-GHz suspended-substrate IF transformers (50–200 Ω). Quartz = 0.15-mm thick, cavity = 1.9-mm square.

to provide the 250- to 50-Ω impedance range and match (at the connector side) to a standard microstrip launcher. Due to some initial moding problems with the connector-to-stripline joint at 20 GHz, the original wide tab (0.050 in) launcher had to be replaced with a 0.020-in-wide tab launcher.[1] A through measurement on two back-to-back 200- to 50-Ω transformers is shown in Fig. 7.

Assembly of the mixer block is fairly simple and can usually be accomplished in less than 1 h. A photo of the assembled mixer (without the backshort cavity and with the top half removed) can be seen as Fig. 8, and a close-up of the membrane mounting is shown as Fig. 9.

IV. Performance

A. Test System

Accurate RF noise measurements at 2.5 THz are complicated by several factors: high mixer noise temperatures, variable atmospheric attenuation, poorly calibrated "absolute power" detectors, unavailability of matched attenuators, "gray body" loads, and imperfect Gaussian beams. The measurement test system used here to overcome these difficulties is shown schematically in Fig. 10. LO power is generated by a compact CO_2-pumped methanol gas laser with a maximum output power of 7 mW at 2522 GHz.[2] A Martin–Puplett-style wire-grid diplexer[3] is used to spatially combine the LO and signal beams. An off-axis ellipsoidal mirror matches the beam of the diplexer to that of the Pickett–Potter feed horn. The laser beam profile at 2.5 THz can be coarsely viewed with low thermal-response liquid-crystal paper and, when the laser is properly tuned, appears to be circular with a single bright central spot. LO power measurement is provided by a "calibrated" Sci-

[1] CDI part numbers 5753 CC or 5763 CC. Available from Connecting Devices, Long Beach, CA 90815.

[2] Laser fabricated by Dr. A. Peebles, Innovative Research and Technology, Santa Monica, CA 90403, under NASA Small Business Innovative Research Grant NAS7-1312.

[3] Diplexer fabricated by Thomas Keating Ltd., Station Mills, Billingshurst, West Sussex RH14-9SH, U.K.

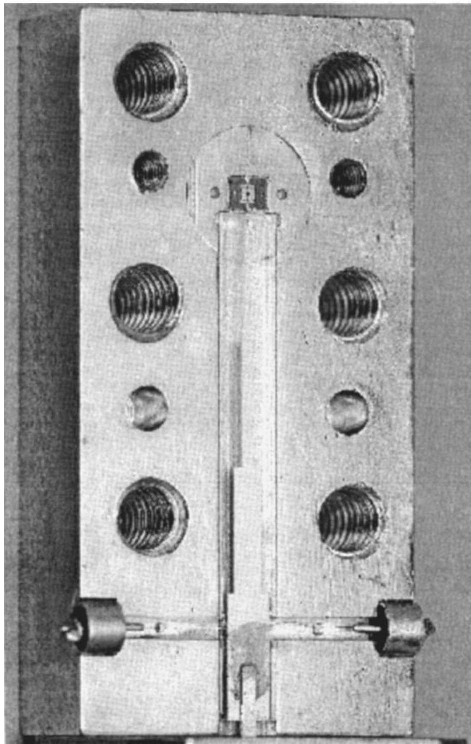

Fig. 8. Photo showing bottom half of complete 2.5-THz mixer block with RF membrane diode, quartz IF transformer, and dc-bias resistor and sensing taps. A backshort tuner cavity and top block seal the membrane and IF transformer cavities.

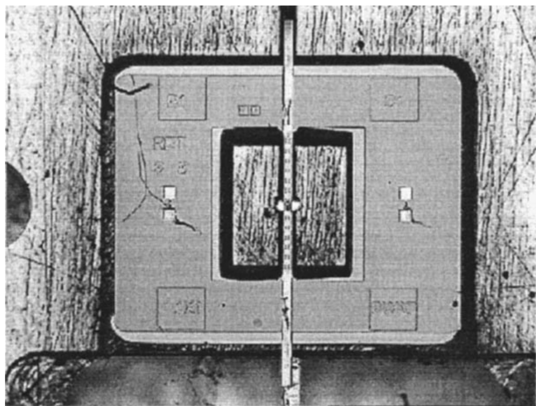

Fig. 9. Close-up showing MOMED mounted in "button" with diode suspended across 2.5-THz waveguide (center), dc return (top), and IF transformer beamlead bond (bottom).

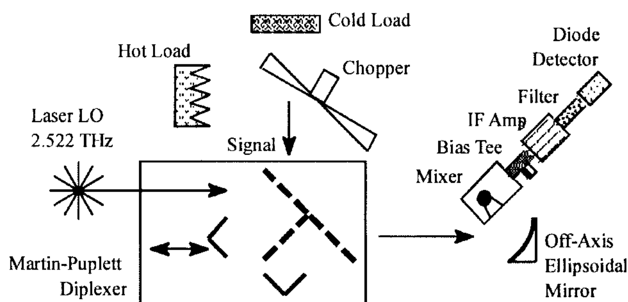

Fig. 10. Schematic of the RF test system used to collect the performance data given in this paper.

entech multimode thermal detector and the numbers reported here should be taken with error bars of at least 3 dB, due to beam mode and detector absorber nonidealities.

The noise temperatures are measured using the standard Y-factor technique on the full receiver only. A chopper switches the signal beam between a hot load (wedged Eccosorb CR110) and a cold load (Eccosorb AN74 flat sheet, soaked in liquid nitrogen), held in the signal beam during the measurement. The assumed hot- and cold-load temperatures are 300 and 77 K, respectively, no corrections are made to account for mismatch or nonideal Rayleigh–Jeans behavior. A lock-in detector at $\approx$100-Hz chopper frequency is used to extract a hot/cold-load power output variation from a crystal diode detector. A correction factor of 0.45 is divided into the lock-in value to convert its root mean square (rms) output to a peak-to-peak value (the chopper bow-tie blade, radius 50 mm, produces a good approximation to a square wave as it switches the relatively small signal beam waist radius of $\approx$4 mm). This peak-to-peak variation is then summed with the dc average diode detector value to give the hot and cold powers needed for an accurate Y-factor measurement. This lock-in technique can be used to evaluate receivers with noise in excess of 500 000-K double sideband (DSB).

For the results reported here, a broad-band bias-T[4] connects the mixer to a low-nose broad-band IF amplifier.[5] The IF amplifier provides approximately 65 dB of gain over the frequency range 7–21 GHz, with noise at the low frequency end of $\approx$150 K, and at the high frequency end of $\approx$200 K. Coaxial filters[6] limit the detected bandwidth to $\approx$700 MHz about the desired center frequencies of 8.4, 12.8, and 20.4 GHz. Detected power is in the neighborhood of 15 μW. Front-end conversion loss is measured using a power meter to calibrate the response of the crystal diode detector and then extracting the measured amplifier gain and filter loss (0.9 dB).

Mixer noise temperature can be extrapolated from the receiver measurements after separate IF amplifier calibration, but includes diplexer, atmospheric, and horn coupling losses as well as any bias-T losses and IF impedance mismatch that may be present between the mixer output port and amplifier. We can provide only approximate corrections for these losses until better calibration can be performed. They are distributed as follows:

diplexer signal loss	0.5 dB;
mirror-to-horn coupling loss	0.5 dB;
bias-T loss	0.4 dB;
IF mismatch loss	up to 3 dB at 21 GHz based on relative IF measurements;
atmospheric losses	1 dB.

More accurate values will be obtained in the future. For this paper, we will not attempt to calibrate out these losses, but will refer to "front-end" (rather than mixer) noise and loss as that belonging to all components forward of the IF amplifier.

[4] Wiltron model K250 bias-T, Wiltron Company, Morgan Hill, CA 95037-2809.

[5] MITEK model JSD2-00010, MITEQ, Inc., Hauppauge, NY 11788.

[6] K&L Microwave Inc., Salisbury, MD 21804.

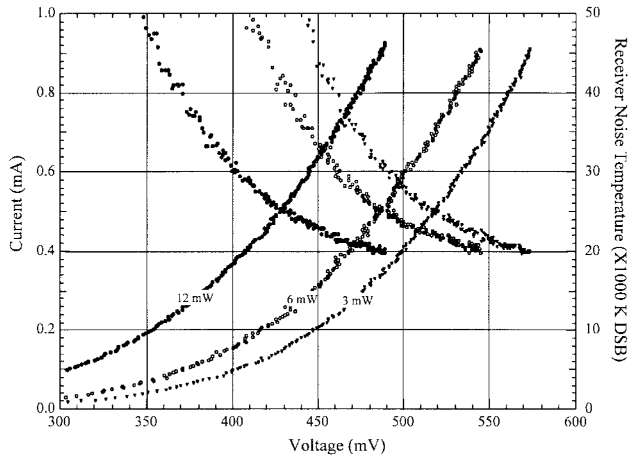

Fig. 11. Measured bias current and receiver noise temperature at 8.4-GHz IF as a function of bias voltage for LO power levels of ≈12, 6, and 3 mW (left-to-right). The bias current curves exhibit monotonic positive slope, noise temperature curves negative.

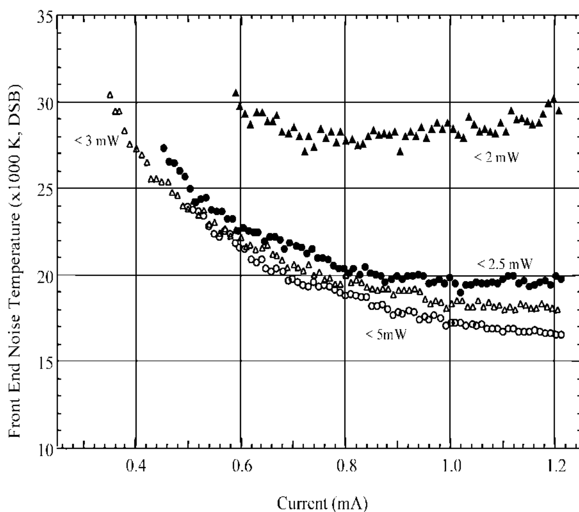

Fig. 12. Measured receiver noise temperature at 8.4-GHz IF for best device to date at LO power levels between <2 and ≈5 mW. The best noise temperature obtained with this device was 16 500-K DSB at ≈5 mW.

During measurements, the mixer is current biased so that LO power fluctuations are compensated by a voltage change on the diode. We find that current bias (≈ curvature bias) makes the mixer relatively insensitive to changes of LO power. On one diode (Fig. 11), we nominally observed the same receiver noise temperature at fixed current when we altered the LO power by more than a factor of five. In Fig. 12, our best device, the LO sensitivity is somewhat higher.

The entire RF noise test system is computer controlled and can be programmed to sweep bias current versus time to obtain the plots shown in the figures. Pumped and unpumped *IV* curves can also be generated. Typically, we operate with a lock-in time constant of 300 ms and 100 data points per curve.

B. Receiver/Mixer Noise

Measured receiver noise temperatures, using the test system described in Section IV, are given in Figs. 11 and 12, plotted against bias voltage in one case and current in the other. The devices that produced these results had measured areas of 0.35×1 μm^2, measured resistances between 15 and 20 Ω, ideality factors of about 1.5, and a saturation current between 0.3 and 2 pA. Smaller area devices have not yielded as good performance. A backshort depth between 15 and 20 μm consistently gave the best performance during tests of several different devices of varying resistance. Thus far, approximately ten devices have been measured, and four have given performance similar to that shown in Fig. 11. As can be seen from the figure, the current bias greatly mitigates the effect of LO power variation. In fact, we were able to adequately pump the mixer with only 3 mW of measured LO power and could occasionally go as low as 2.5 mW without noticeably starving the diode. On the other extreme, pump power levels as high as 22 mW did not burn out the device and we could obtain essentially identical noise temperature versus bias current curves for the two LO power extremes.

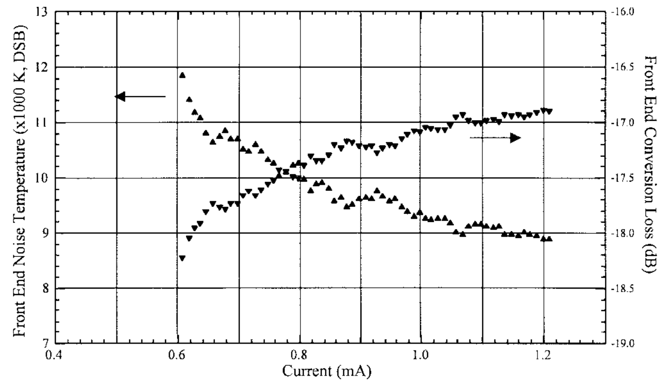

Fig. 13. Extrapolated "front-end" (diplexer, feed mirror, mixer, bias-T) noise temperature and conversion loss at 8.4-GHz IF as a function of mixer bias current at a fixed LO power of ≈6 mW. No corrections for air losses or Rayleigh–Jeans approximation have been included. The minimum noise temperature is ≈9000-K DSB, and the minimum front-end conversion loss is ≈16.9 dB.

Fig. 12 shows the effect of LO power on the performance of our best device measurement to date. Power is measured by an infrared (IR) calibrated Scientech power meter placed in front of the RF diplexer. A best receiver performance of 16 500 K was recorded at an LO power of approximately 6 mW. The "front-end" noise and conversion loss for this same device, extracting the amplifier noise of 150 K, are shown in Fig. 13; again, as a function of bias current at fixed LO power. No corrections are made for diplexer, mirror, horn, bias-T, or air losses. The best performance is obtained with 1.2-mA bias current in the diode and measures less than 9000-K DSB noise temperature and 16.9-dB conversion loss for the front-end. All the data shown is at an IF of 8.4 GHz. At 12.8 GHz (on a different, but similarly performing device), the receiver noise is within 10% of 8.4 GHz, but at 20.4 GHz, the noise performance is a factor of two higher for all devices. Recent experiments suggest that the connection between the SMA tab launcher and the IF filter is responsible for this degradation and it is easily fixed with additional wire bonds.

The mixer performance is sensitive to the backshort cavity depth; changes of as little as 10 μm can result in changes of more than 50% in receiver noise. This is consistent with the sensitivity observed in lower frequency mixers that use full height waveguide.

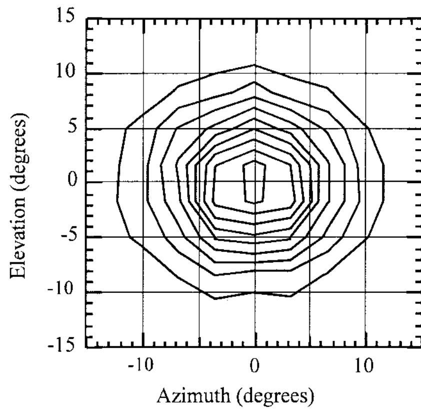

Fig. 14. Measured beam pattern of 2.5-THz Pickett–Potter feed horn using the LO pump laser as the RF source and the mixer as a direct detector. The contours are linearly spaced in 10% intervals (i.e., the outer contour has 0.1 times the signal strength of the peak).

Thus far, we have measured only a small number of membrane devices and have not accumulated enough data to make any conclusions regarding the importance of the device dc parameters on RF performance. A large change in optimal backshort cavity depth was observed between the 0.2×1 and 0.35×1 μm^2 area diodes, with the smaller diodes requiring more matching inductance (larger cavity depth), but a more detailed analysis on the full RF circuit has not yet been concluded. Further measurements on devices with different doping and epilayer profiles, anode areas, and RF circuit configuration are clearly desirable and in progress.

C. RF Beam Pattern

As a final characterization measurement, we used the mixer as a direct detector to measure the beam pattern of the Pickett–Potter feed horn. The data is presented in Fig. 14. The laser-beam quality allowed us to reliably measure only to the 10-dB level, but the beam widths at this and the 3-dB point match those predicted in [24].

V. Summary

A novel GaAs membrane diode circuit concept has been developed and demonstrated. The membrane fabrication process has been combined with our existing submillimeter-wave planar T-anode mesa Schottky diode process to design and fabricate a 2.5-THz waveguide mixer. Early measurements of mixer performance have shown the design to be competitive with alternative corner-cube and whisker-contacted waveguide mixer concepts, although not as good as the best reported measurements in the literature. In addition, the required LO power is as low as 6 mW (optimal) and 3 mW slightly starved. The membrane devices have proven to be both robust and reliable, having been taken through "shake and bake" with no mechanical failure. The waveguide block, although requiring careful machining and electroforming, is relatively simple to fabricate and assemble. The combination of the narrow membrane bridge circuit, containing both the integrated planar diode and RF filters, allows the implementation of sealed-cavity single-mode circuitry everywhere, even at wavelengths as short as 100 μm. The membrane fabrication process requires no post processing on the die as chemical etching replaces labor-intensive dicing or scribe and break procedures. The lack of induced stress on the completed membrane makes it ideal for circuits where long thin bridging is required. The circuit and device implementation demonstrated in this application can be employed for other submillimeter- and millimeter-wave components including multipliers or harmonic mixers (membrane couples to two different-size waveguides), heterodyne arrays (multiple membranes superimposed on a feed-horn array), oscillators (cavity-coupled membrane strip) or micromachined components (membranes used to span formed waveguides or cavities). The circuit described in this paper is being employed on a NASA flight mission and will undergo extensive lifetime and reliability screening before delivery of finished components.

Acknowledgment

The authors would like to acknowledge the many valuable contributions of P. Bruneau to the mixer block fabrication process. They would also like to thank J. Podosek for device fabrication support, J. Oswald for help in setting up the FDTD analysis of the RF filters, A. Pease and R. Lin for the device thermal cycling, R. Tsang for device sorting and testing, T. Lee for the IF transformer processing and U. Zimmermann for IF transformer measurements. Finally, the authors would like to acknowledge the concept brought to their attention by C. Mann, Rutherford Appleton Laboratories, Didcot, U.K., from which the circuit described in this paper is derived. This work was carried out at the California Institute of Technology Jet Propulsion Laboratory, Pasadena, CA.

References

[1] G. V. Eleftheriades, W. Y. Ali-Ahmed, and G. M. Rebeiz, "Progress in integrated circuit horn antennas for receiver applications: Part I and II," in *2nd Int. Symp. Space THz Technol.*, Pasadena, CA, Mar. 24–26, 1992, pp. 324–344.

[2] J. W. Kooi, M. S. Chan, P. Schaffer, B. Bumble, H. G. LeDuc, C. K. Walker, and T. G. Phillips, "An 850 GHz waveguide receiver using tuned Nb SIS tunnel junction fabricated on a 1 μm Si_3N_4 membrane," in *7th Int. Symp. Space THz Technol.*, Charlottesville, VA, Mar. 12–14, 1996, pp. 86–102.

[3] G. de Lange, B. R. Jackson, A. Rahman, E. Duerr, and Q. Hu, "Low-noise micromachined SIS mixers for millimeter-wave imaging arrays," in *7th Int. Symp. Space THz Technol.*, Charlottesville, VA, Mar. 12–14, 1996, pp. 29–36.

[4] R. F. Drayton, C. Kidner, J. East, and L. P. B. Katehi, "Micromachined detector mounts for millimeter-wave applications," in *5th Int. Symp. Space THz Technol.*, Ann Arbor, MI, May 10–12, 1994, pp. 796–801.

[5] T. Weller, S. Robertson, L. P. Katehi, and G. M. Rebeiz, "Millimeter and submillimeter wave microshield line components," in *5th Int. Symp. Space THz Technol.*, Ann Arbor, MI, May 10–12, 1994, pp. 802–810.

[6] C.-Y. Chi and G. M. Rebeiz, "Planar microwave and millimeter-wave lumped elements and coupled-line filters using micromachining techniques," *IEEE Trans. Microwave Theory Tech.*, vol. 43, pp. 730–38, Apr. 1995.

[7] K. Hjort, "Sacrificial etching of III–V compounds for micromechanical devices," *J. Micromech. Microeng.*, vol. 6, no. 4, pp. 370–375, Dec. 1996.

[8] A. Dehe, D. Pavlidis, K. Hong, and H. L. Hartnagel, "InGaAs/InP thermoelectric infrared sensor utilizing surface bulk micromachining technology," *IEEE Trans. Electron Devices*, vol. 44, pp. 1052–1059, July 1997.

[9] Y. Uenishi, H. Tanaka, and H. Ukita, "AlGaAs/GaAs micromachining for monolithic integration of micromechanical structures with laser diodes," *IEICE Trans. Electron.*, vol. E78-C, no. 2, pp. 139–145, Feb. 1995.

[10] C. Seassal, J. L. Leclercq, and P. Viktorovitch, "Fabrication of InP-based freestanding microstructures by selective surface micromachining," *J. Micromech. Microeng.*, vol. 6, no. 2, pp. 261–265, June 1996.
[11] C. I. Lin, A. Simon, M. Rodriguez-Gironies, H. L. Hartnagel, P. Zimmermann, and R. Zimmerman, "Substrateless Schottky diodes for THz applications," in *8th Int. Symp. Space THz Technol.*, Cambridge, MA, Mar. 25–27, 1997, pp. 224–229.
[12] R. P. Smith, S. C. Martin, M. Kim, J. Bruston, D. Humphrey, N. Erickson, and P. H. Siegel, "Advances in submillimeter wave semiconductor-based device designs and processes," in *8th Int. Symp. Space THz Technol.*, Cambridge, MA, Mar. 25–27, 1997, pp. 184–197.
[13] S. Allen, M. Reddy, M. J. W. Rodwell, R. P. Smith, S. C. Martin, J. Liu, and R. Muller, "Submicron Schottky-collector AlAs/GaAs resonant tunnel diodes," in *IEEE Int. Electron Devices Meeting*, Wash. D.C., Dec. 1993, pp. 407–410.
[14] R. E. Muller, S. C. Martin, R. P. Smith, S. A. Allen, M. Reddy, U. Bhattacharya, and M. J. W. Rodwell, "Electron beam lithography for the fabrication of air-bridged, submicron Schottky collectors," *J. Vac. Sci. Technol. B, Microelectron. Process. Phenom.*, vol. 12, no. 6, Nov.–Dec. 1994.
[15] W. Bishop, K. McKinney, R. Mattauch, T. Crowe, and G. Green, "A novel whiskerless diode for millimeter and submillimeter wave applications," in *IEEE MTT-S Int. Microwave Sym. Dig.*, June 1987, pp. 607–610.
[16] H. Krautle, E. Sauter, and G. V. Schultz, "Properties of a submillimeter mixer in an open structure configuration," *Infrared Phys.*, vol. 18, pp. 705–712, 1978.
[17] J. Zmuidzinas, A. L. Betz, and R. T. Boreiko, "A corner-reflector mixer mount for far infrared wavelengths," *Infrared Phys.*, vol. 29, no. 1, pp. 119-131, 1989.
[18] H. W. Hubers, T. W. Crowe, G. Lundershausen, W. C. B. Peatman, and H. P. Roser, "Noise temperature and conversion losses of submicron GaAs Schottky-barrier diodes," in *4th Int. Symp. Space THz Technol.*, Los Angeles, CA, Mar. 30–Apr. 1, 1993, pp. 522–527.
[19] A. L. Betz and R. T. Boreiko, "A practical Schottky mixer for 5 THz," in *6th Int. Symp. Space THz Technol.*, Pasadena, CA, Mar. 21–23, 1995, pp. 28–33.
[20] B. N. Ellison, B. J. Maddison, C. M. Mann, D. N. Matheson, M. L. Oldfield, S. Marazita, T. W. Crowe, P. Maaskant, and W. M. Kelly, "First results for a 2.5 THz Schottky diode waveguide mixer," in *7th Int. Symp. Space THz Technol.*, Charlottesville, VA, Mar. 12–14, 1996, pp. 494–502.
[21] C. Mann, private communication.
[22] S. W. Moon, C. M. Mann, B. J. Maddison, I. C. E. Turcu, R. Allot, S. E. Huq, and N. Lisi, "Terahertz waveguide components fabricated using a 3D X-ray microfabrication technique," *Electron. Lett.*, vol. 32, no. 19, pp. 1794–1795, Sept. 1996.
[23] J. E. Oswald, P. H. Siegel, and S. Ali, "Finite difference time domain analysis of coplanar transmission line circuits and a post gap waveguide mounting structure," in *5th Int. Symp. Space THz Technol.*, Ann Arbor, MI, May 10–12, 1994.
[24] H. M. Pickett, J. C. Hardy, and J. Farhoomand, "Characterization of a dual mode horn for submillimeter wavelengths," *IEEE Trans. Microwave Theory Tech.*, vol. MTT-32, pp. 936–938, Aug. 1984.

Peter H. Siegel (S'77–M'83–SM'98) was born in New Rochelle, NY, in 1954. He received the undergraduate degree from Colgate University, Hamilton, NY, in 1976, and the M.Sc. and Ph.D. degrees in electrical engineering from Columbia University, New York, in 1978 and 1983, respectively.

He began his career in 1975 working on millimeter-wave mixers and multipliers at the NASA Goddard Space Flight Center, Institute for Space Studies, New York. In 1984, he moved to the Central Development Laboratory, National Radio Astronomy Observatory, where he spent three years working on millimeter receivers for the NRAO Kitt Peak 12-m telescope. He joined the Advanced Devices Group, California Institute of Technology, Jet Propulsion Laboratory (JPL), Pasadena, CA, in 1989. In 1994, he formed the JPL Submillimeter Wave Advanced Technology (SWAT) team, which he supervises. The group is currently composed of approximately 25 engineers and scientists who provide technology development and instrumentation support for NASA's advanced millimeter and submillimeter-wave missions. His research interests include millimeter- and submillimeter-wave devices, components, and subsystems.

R. Peter Smith was born in Hartford, CT, in 1955. He received the B.Sc. degree in physics from Bates College, Lewiston, ME, in 1977, and the M.Sc. and Ph.D. degrees from Brown University, Providence, RI, in 1982 and 1986, respectively.

From 1986 to 1990, he was with GE Electronics Laboratory, Syracuse, NY. He is currently with the California Institute of Technology, Jet Propulsion Laboratory, Pasadena, CA. His current research interests include a number of high-speed electronic devices and related circuits. He is currently working on submillimeter-wave mixer and multiplier device and circuit development, millimeter-wave grid amplifiers using HEMT's, and other III–V devices and integration approaches. He is also currently focusing on optimizing processes and devices for operation at frequencies greater than 200 GHz.

Michael C. Gaidis was born in Madison, WI, on March 10, 1967. He received the B.S. degrees in physics and electrical engineering, and the M.S. degree in electrical engineering from the Massachusetts Institute of Technology, Cambridge, in 1989, and the Ph.D. degree in applied physics from Yale University, New Haven, CT, in 1994.

He served as a Post-Doctoral Research Fellow at the California Institute of Technology, Pasadena, CA, until 1995, and was then with the Jet Propulsion Laboratory (JPL), Pasadena, CA, as a Staff Member involved with superconducting hot electron bolometers. He is currently a Cognizant Engineer at JPL, where he is responsible for delivering a 2.5-THz receiver front end to the EOS-MLS satellite instruments.

Suzanne C. Martin (S'89–A'90) received the B.S. and M.S. degrees in electrical engineering from Brown University, Providence, RI, in 1985 and 1991, respectively.

From 1985 to 1989, she was a Research Engineer at Brown University, where she designed and fabricated germanium photodiodes and metal–oxide–semiconductor field-effect transistors (MOSFET's). She is currently a member of the Engineering Staff at the California Institute of Technology, Jet Propulsion Laboratory, where she is involved in the fabrication of mixer and varactor diodes for submillimeter-wave applications along with e-beam process development for other devices including HEMT's, heterojunction bipolar transistors (HBT's), and GaN FET's.